Mon. Not. R. Astron. Soc. **360,** 1493–1505 (2005) doi:10.1111/j.1365-2966.2005.09142.x

Rotational evolution of protoneutron stars with hyperons: spin up or not?

Y.-F. Yuan[1⋆] and Jeremy S. Heyl[2,3⋆†]

[1]*Center for Astrophysics, University of Science and Technology of China, Hefei, Anhui 230026, China*
[2]*Harvard-Smithsonian Center for Astrophysics, Cambridge, MA 02138, USA*
[3]*Department of Physics and Astronomy, University of British Columbia 6224 Agricultural Road, Vancouver, BC, Canada, V6T 1Z1*

Accepted 2005 April 20. Received 2005 April 20; in original form 2005 February 10

ABSTRACT

We study the evolution of a rigidly rotating protoneutron star (PNS) with hyperons and nucleons or solely nucleons in its core due to the escape of trapped neutrinos. As the neutrinos escape, the core nucleonic neutron star (NS) expands and the stellar rotation slows. After the neutrinos escape, the range of the spin periods is narrower than the initial one, but the distribution is still nearly uniform. A PNS with hyperons, at the late stage of its evolution, keeps shrinking and spinning up until all the trapped neutrinos escape. Consequently, the distribution of the stellar initial spin periods is skewed towards shorter periods. If the hyperonic star is metastable, its rotational frequency accelerates distinguishedly before it collapses to a black hole.

Key words: dense matter – stars: evolution – stars: neutron – stars: rotation.

1 INTRODUCTION

A neutron star (NS) is born after the collapse of the iron core of a massive star ($>M_{\odot}$) that exhausts its nuclear fuel. The birth of the NS is often associated with a core-collapse supernova explosion (Burrows 2000; Janka, Kifonidis & Rampp 2001). Immediately after its birth, the NS is hot and lepton-rich because the core is opaque to neutrinos. This young object is called a protoneutron star (PNS). Since the seminal work by Burrows & Lattimer (1986), non-rotating PNSs have been studied in detail (Keil & Janka 1995; Pons et al. 1999, 2001a,b). Previous works have shown that as compared with the neutrino-free case (i.e. the cold NS), the trapped neutrinos significantly change the chemical equilibria between baryons and leptons, the fractions of all the compositions, and the equation of state (EOS); therefore, the Kelvin–Helmholtz epoch of the evolution of the PNS, during which the PNS changes from a hot and lepton-rich compact star to a cold and neutrino-free one, is the most important evolutionary stage of the PNS. The time-scale of the Kelvin–Helmholtz epoch completely depends on the neutrino interactions in the hot and dense matter (Reddy, Prakash & Lattimer 1998). Namely the diffusion time-scale of the trapped neutrinos from the core to the outside is roughly several tens of seconds (Prakash et al. 1997). As pointed out in the literature, in principle, observations of supernova neutrinos may constrain the EOSs and the interior composition of NSs (Prakash, Cooke & Lattimer 1995; Pons et al. 1999, 2001a,b).

After its birth, the NS generally spins fast initially, even near to the Keplerian angular velocity, $\Omega_{\rm K}$ (Fryer & Heger 2000; Heger, Langer & Woosley 2000). Stellar rotation is essential for the generation of the magnetic field (e.g. Thompson & Duncan 1993) and affects the global properties of the PNS significantly (Akiyama et al. 2003). In order to deal with the rotation of a rapidly rotating PNS, a fully general relativistic method should be used. However, this is a formidable task. One of the main difficulties stems from the complexity of the neutrino transport in more than one dimension. On the other hand, the Kelvin–Helmholtz time-scale over which the neutrinos escape ($\sim$10 s) is much longer than the dynamical time-scale of the PNS ($\sim$1 ms), therefore, the temporal sequence of quasi-equilibrium models of PNS has been analysed under several simplified assumptions: the conservation of baryons, conservation of angular momentum, the constant temperature or constant entropy profile of the hot dense matter, the constant neutrino fraction and so on (Romero et al. 1992; Goussard, Haensel & Zdunik 1997, 1998; Strobel, Schaab & Weigel 1999; Villain et al. 2004). Under these assumptions, we simplify the rotational evolution of PNS by studying a stationary axisymmetric space–time with a rigidly rotating perfect fluid. Stergioulas (1998) outlines several independent techniques to solve Einstein's equation for this situation. The most up-to-date investigation of this problem can be found in (Villain et al. 2004): in their analysis, the authors used the realistic temperature and chemical profiles coming from 1D simulations (Pons et al. 1999) and included differential rotation.

The properties of PNSs that contain only ordinary nuclear matter have been investigated in detail by many authors (Hashimoto, Oyamatsu & Eriguchi 1994; Takatsuka, Nishizaki & Hiura 1994; Bombaci et al. 1995; Goussard et al. 1997; Prakash et al. 1997; Goussard et al. 1998; Strobel et al. 1999; Sumiyoshi, Ibáñez & Romero 1999). Because of the uncertainties of the composition of the matter in the interior of

⋆E-mail: yfyuan@ustc.edu.cn (Y-FY); heyl@physics.ubc.ca (JSH)
†Chandra Fellow, Canada Research Chair.

NSs, the effects of some exotic states, such as hyperonic matter (Prakash et al. 1997; Pons et al. 1999), quark matter (Pons et al. 2001b), kaon condensation (Pons et al. 2001a) and the quark–hadron phase transition (Prakash et al. 1995), on the evolution of PNSs have also been explored. Because the trapped neutrinos increase the chemical potential of electrons, the common consequence of the inclusion of the possible exotic states that contain negatively charged components in the PNS is the existence of a metastable star, the mass of which is larger than the maximum mass for a cold neutrino-free NS (Prakash et al. 1997). Inevitably, the metastable PNS will collapse to a black hole at some time during the Kelvin–Helmholtz epoch. Meanwhile, the neutrino signal from the PNS will cease suddenly, because the time-scale of the collapse is of the order of the free-fall time, which is much shorter than the evolutionary time-scale of the PNS (Pons et al. 1999, 2001a,b).

As the trapped neutrinos escape, the global structure of the PNS changes, especially the moment of inertia; this affects the stellar rotational frequency dramatically. In this work, we study the evolution of PNSs by assuming that they evolve through a series of hydrostatic equilibria with successively smaller neutrino fractions that are assumed to be constant in the neutrino opaque core: that is, we investigate the stellar global properties as a function of the number density of the trapped electron neutrinos. Especially, we contrast the rotational evolution of hyperonic PNSs with ordinary PNSs to check whether the PNS with hyperons spins up at the end of its Kelvin–Helmholtz epoch. The evolutionary behaviour of a PNS in whose core the other possible exotic states exist is qualitatively similar to the results for the hyperonic star. In order to describe the hyperonic matter with trapped neutrinos, the relativistic mean field theory (RMFT) has been generally applied (Walecka 1974; Chin 1977; Serot 1979; Serot & Walecka 1986; Müller & Serot 1996; Prakash et al. 1997; Yuan & Zhang 1999; Glendenning 2000). The potential model is also used sometimes (Prakash et al. 1997). Recently, the potential model with the Bruecker–Bethe–Goldstone many-body theory at zero temperature was employed to model the hyperonic matter with trapped neutrinos and to investigate the global properties of the PNSs. As expected, the qualitative results that have been obtained in both the models are very similar (Vidaña et al. 2003). The previous works have indicated that the effect of the trapped neutrinos dominates over that of temperature on the internal composition and EOS (Prakash et al. 1997). Thus, for simplicity, we use the RMFT to describe the dense nuclear matter with hyperons at zero temperature and explore the response of the rotational frequency to the escape of the neutrinos. A brief introduction to RMFT for dense matter with hyperons can be found in Appendix A.

This paper is organized as follows. The microscopic properties of dense matter in β equilibrium, and the global properties of the non-rotating and rapidly rotating PNSs are given in Section 2. In Section 3, the numerical results of the evolution of the rotational frequency are presented. The results and discussion will be given in Section 4.

2 PROPERTIES OF NON-ROTATING AND ROTATING PNSS

2.1 The interior composition and the EOS

As the neutrinos escape, their fraction relative to the baryons $Y_{\nu_e} \equiv n_{\nu_e}/n_B$ decreases with time. Because our purpose in this work is to explore the rotational behaviour of the PNS as the neutrinos escape, we study the rotational frequency and other interesting quantities as a function of Y_{ν_e}. The ratio of the number fraction of electron neutrinos to its initial value ($f_{\nu_e} = Y_{\nu_e}/Y^{i}_{\nu_e}$) is assumed to be a constant with baryon number density in the neutrino opaque core, for a given time. Because the density in the stellar core is almost constant, this is a good approximation. As the electron neutrinos escape, the muon neutrino appears due to the following reaction,

$$e^- \rightarrow \mu^- + \overline{\nu}_\mu + \nu_e. \quad (1)$$

To describe the escape of the muon neutrinos, we assume that the ratio of the net number of the escaped muon antineutrinos to that of the muon antineutrinos that should escape freely if the matter is transparent to neutrinos equals to f_{ν_e}. Our calculations show the net number density of muons is generally several orders of magnitude lower than that of electrons, so its effects on the EOS of PNS could be neglected, even though we have taken it into consideration.

The region of the trapped neutrinos ($n_B > n_{env}$) is called the neutrino ellipsoid (or neutrinosphere); its location is determined by the optical depth of neutrinos in the hot stellar mantle (e.g. Goussard et al. 1997). Due to the complexities of neutrino–matter interactions, there is no consensus on the value of n_{env} in the literature. For instance, the suggested values might be $n_{env} \simeq 6 \times 10^{-6}$ fm^{-3} (Hashimoto et al. 1994), $n_{env} \simeq 8 \times 10^{-2}$ fm^{-3} (Bombaci et al. 1995), $n_{env} \simeq 5 \times 10^{-3}$ fm^{-3} (Goussard et al. 1997) and $n_{env} \simeq 6 \times 10^{-4}$ fm^{-3} (Strobel et al. 1999). In this work, we treat n_{env} as a free parameter and choose the latter modest value, i.e. $n_{env} \simeq 6 \times 10^{-4}$ fm^{-3}. Before the neutrinos escape, we set $Y_{L_e} = 0.4$ inside the neutrino ellipsoid, below the density of the neutrino ellipsoid, we simply assume $Y_\nu = 0$. For the description of neutrino-free subnuclear matter, the Friedman and Pandharipande Skyrme Model (FPS) EOS (Lorenz, Ravenhall & Pethick 1993) is chosen, which is smoothly matched to the EOS of nuclear matter described in RMFT. At low baryon number density ($n_B < 0.1$ fm^{-3}), the nucleons are non-relativistic, thus the pressure contributed by the trapped neutrinos and the relativistic electrons dominates. The EOS of subnuclear density matter becomes much stiffer due to the trapped neutrinos.

The thermal effects are neglected in this work; therefore, we will qualitatively discuss the influence of the thermal effects under different possible values of n_{env}. If the thermal effects are introduced, in the inner core, the Fermi energy of particles is much larger than their thermal energy, therefore, temperature has little effect on the global properties such as stellar masses, luminosities, average temperatures of the average lepton content and so on. However, in the outer layers, the EOS becomes much stiffer than in the zero-temperature case; therefore, the stellar radii are greatly larger than those in zero temperature case. A PNS of baryon mass $M_0 = 1.5\,M_\odot$ with a hot envelope has an initial radius of approximately $R_{hot} = 50$–100 km, and the corresponding radius of the star with a cold envelope is approximately $R_{cold} = 18$ km, if n_{env} is taken to be 5×10^{-3} fm^{-3} as in Goussard et al. (1997), the gravitational mass of the stellar mantle is approximately $6.5 \times 10^{-3}\,M_\odot$, therefore,

the ratio of the moment of inertia of the hot envelope to the total stellar one is approximately given by

$$\frac{I_{\rm env}}{I_{\rm tot}} \simeq \frac{M_{\rm env}}{M}\frac{R^2_{\rm hot}}{R^2_{\rm cold}} \simeq (8\text{–}31) \times \frac{M_{\rm env}}{M} \simeq 4\text{–}15\,\text{per cent}. \quad (2)$$

After mantle contraction, which takes place during approximately the first 0.5 s during the fast cooling of the hot envelope, the angular velocity of the star should increase by 4–15 per cent (the loss of the angular momentum of the envelope is less than 10 per cent of its initial value, which could be neglected). The change of the total moment of inertia is less than 10 per cent, due to the response of the EOS to neutrino escaping. From this observation, the mantle contraction dominates the evolution of the angular velocity (Goussard et al. 1997; Villain et al. 2004). However, in this work, we assume $n_{\rm env} = 6 \times 10^{-4}$ fm^{-3} (Burrows, Hayes & Fryxell 1995; Strobel et al. 1999), in this case, $M_{\rm env} = 6.3 \times 10^{-4}\,{\rm M}_\odot$; therefore, $I_{\rm env}/I_{\rm tot} \simeq 0.4$–1.5 per cent before the cooling of the envelope. Thus the effects of the mantle contraction could be neglected, on the other hand, the ignorance of the thermal effects does not qualitatively change the evolution of the stellar angular velocity in our scenario.

The main effect of neutrino trapping in the dense matter above nuclear density is that the fraction of electrons increases dramatically, regardless of the interior composition; therefore, for a PNS that contains only nucleons in its core, the fraction of protons is forced to increase in the same manner because of charge neutrality. Comparing to the neutrino-free case, the symmetry energy, which is contributed by the ρ meson and linearly depends on the difference between the baryon number density of neutrons and protons, decreases significantly (see equations A8 and A12–A13). Consequently, the EOS in the normal stellar core is softer with trapped neutrinos than without them. For hyperonic matter, the higher chemical potential of electrons that results from trapped neutrinos increases the critical baryon number density of the appearance of Σ^- particles. Because there are fewer species of baryons, the Fermi momenta of each species is larger, so the pressure of hyperonic matter with trapped neutrinos is larger than the pressure without neutrinos.

The responses of the EOSs based on the hyperon model (NPH) and nucleon model (NP) as the neutrinos escape are shown in Fig. 1. In the NP model, as expected, the EOSs become more and more stiff as the neutrinos escape. The same occurs in the NPH model, below the critical density of the emergence of the hyperons. However, in the NPH model, at densities above the critical density, the EOSs become softer due to the appearance of the more and more additional components.

2.2 Properties of the non-rotating and rapidly rotating PNSs

In order to solve the Einstein field equations with the source terms, NS matter is generally assumed to behave as a perfect fluid. For a static NS, the resulting equations are well known: the Tolman–Oppenheimer–Volkoff equations. It is complicated to deal with the rotation of an NS. If the stellar angular velocity Ω is small compared with the critical value $\Omega_{\rm c} = \sqrt{4\pi G\epsilon_{\rm c}}$, where $\epsilon_{\rm c}$ is the mass density at the centre of the

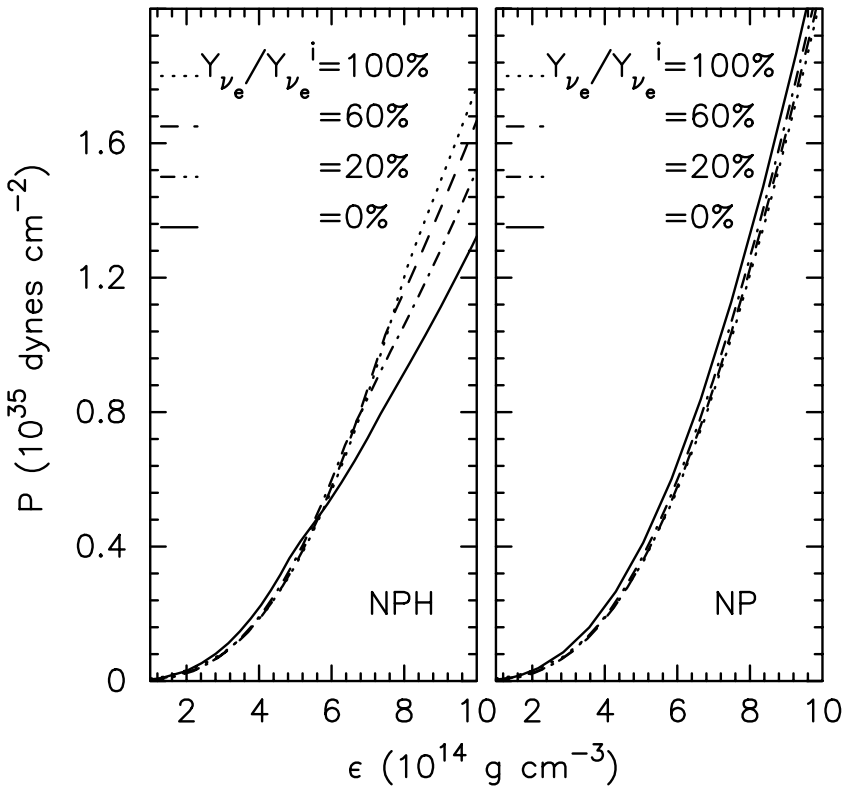

Figure 1. The change of the EOSs of the hyperonic matter (left-hand panel) and the normal nuclear matter (right-hand panel) due to the escape of the neutrinos.

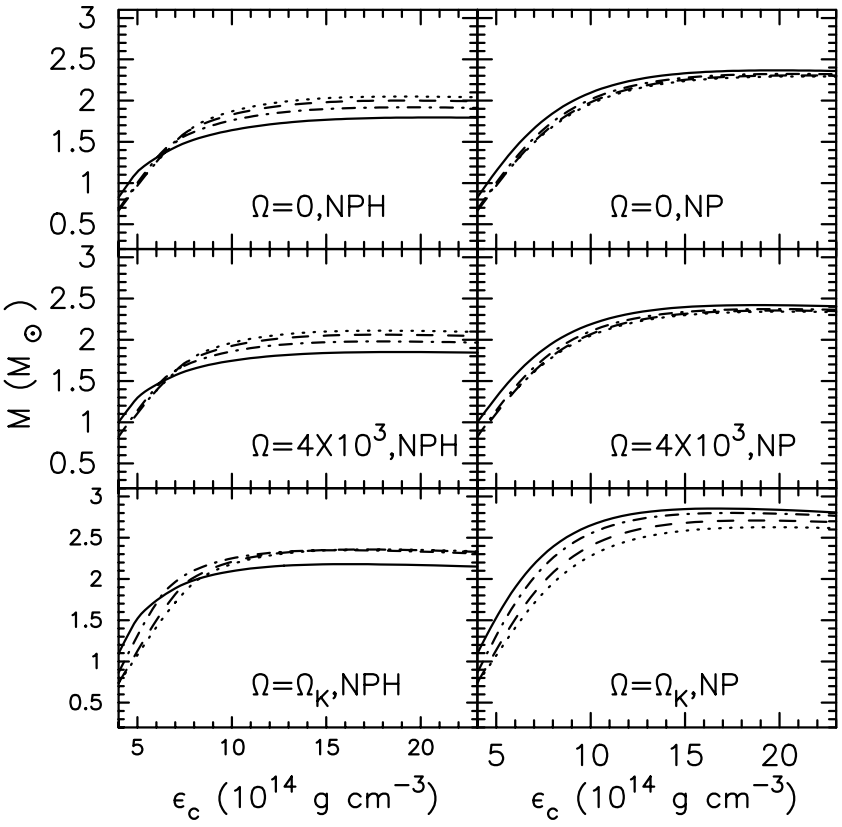

Figure 2. The gravitational mass M as a function of the central density at the different rotation frequencies $\Omega = 0$, $\Omega = 4 \times 10^3\ \mathrm{s}^{-1}$, $\Omega = \Omega_\mathrm{K}$. Left-hand panels are the results for hyperonic matter, while right-hand panels are for the nuclear matter. The solutions traced by the various lines are the same as in Fig. 1, which represent the different values of $Y_{\nu_\mathrm{e}}/Y^\mathrm{i}_{\nu_\mathrm{e}}$.

star, the perturbation theory developed by Hartle and Thorne is accurate enough (Hartle 1967; Hartle & Thorne 1968; Chubarian et al. 2000). Hartle's original perturbation theory was improved by considering the effects of centrifugal stretching and frame dragging in an attempt to calculate the properties of a rapidly rotating NS with $\Omega \sim \Omega_\mathrm{c}$ (Glendenning 1992; Weber & Glendenning 1992). Nevertheless, the exact treatment of the rotation of a compact star should be done in full general relativity. Several reasonable assumptions are generally made: they are, the space–time and the matter are stationary and axisymmetric, and the star uniformly rotates. Under these assumptions, the metric of the space–time can be expressed by

$$\mathrm{d}s^2 = e^{\gamma+\rho}\,\mathrm{d}t^2 + e^{2\alpha}(\mathrm{d}r^2 + r^2\mathrm{d}\theta^2) + e^{\gamma-\rho}r^2\sin^2\theta(\mathrm{d}\phi - \omega\mathrm{d}t)^2, \tag{3}$$

where the metric potentials γ, ρ, ω and α are functions of r and θ only. Several independent methods to numerically calculate the metric potentials exist (Stergioulas 1998). Our calculation is based on the Stergioulas & Friedman KEH code (Komatsu, Eriguchi & Hachisu 1989a,b), which is available in the public domain code (Stergioulas & Friedman 1995).[1] After solving the metric potentials, any coordinate-invariant physical quantity can be calculated. For instance, the gravitational mass and the total angular momentum are given as follows:

$$M = 2\pi\int e^{2\alpha+\gamma}\left[\frac{\epsilon+p}{1-v}(1+v^2+2r\omega e^{-\rho}v\sin\theta) + 2p\right]r^2\,\mathrm{d}r\sin\theta\,\mathrm{d}\theta, \tag{4}$$

$$J = 2\pi\int e^{2\alpha+\gamma-\rho}\frac{(\epsilon+p)v}{1-v^2}r^3\,\mathrm{d}r\sin^2\theta\,\mathrm{d}\theta, \tag{5}$$

where $v = re^{-\rho}(\Omega-\omega)\sin\theta$ is the relative velocity between the fluid and the locally non-rotating observer, ϵ and p are the energy density and pressure of the fluid, respectively.

Figs 2–4 show the global properties of the NSs. In Fig. 2, we plot the gravitational mass (M) as a function of the central energy density (ϵ_c) for PNSs with different fractions of trapped neutrinos $f_{\nu_\mathrm{e}} = Y_{\nu_\mathrm{e}}/Y^\mathrm{i}_{\nu_\mathrm{e}}$ and with different rotational frequencies $\Omega = 0$, $\Omega = 4 \times 10^3\ \mathrm{s}^{-1}$ and $\Omega = \Omega_\mathrm{K}$ in both the NP and NPH model. As predicted in the previous works, the maximum mass of the static PNS decreases as the neutrinos escape in the NPH model, which results in the possible existence of a metastable star. In the NP model, the maximum mass increases as the neutrinos escape. These results hold even when the PNS spins very rapidly.

[1] http://www.gravity.phys.uwm.edu/rns/

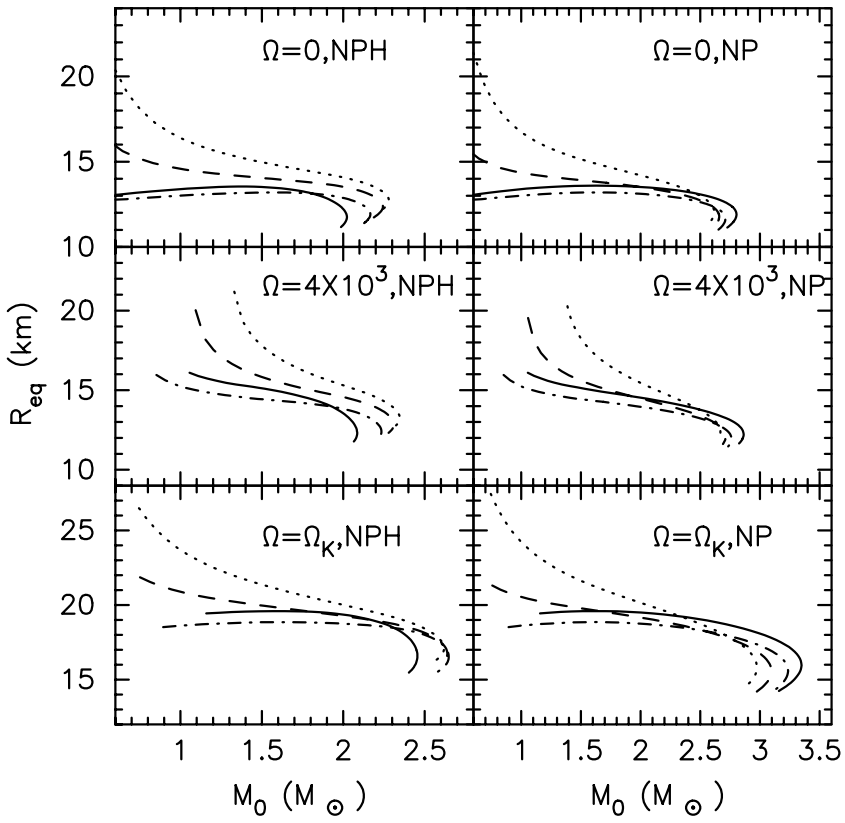

Figure 3. The stellar circumferential equatorial radii as a function of the baryonic mass. The solutions traced by the various lines are the same as in Fig. 1.

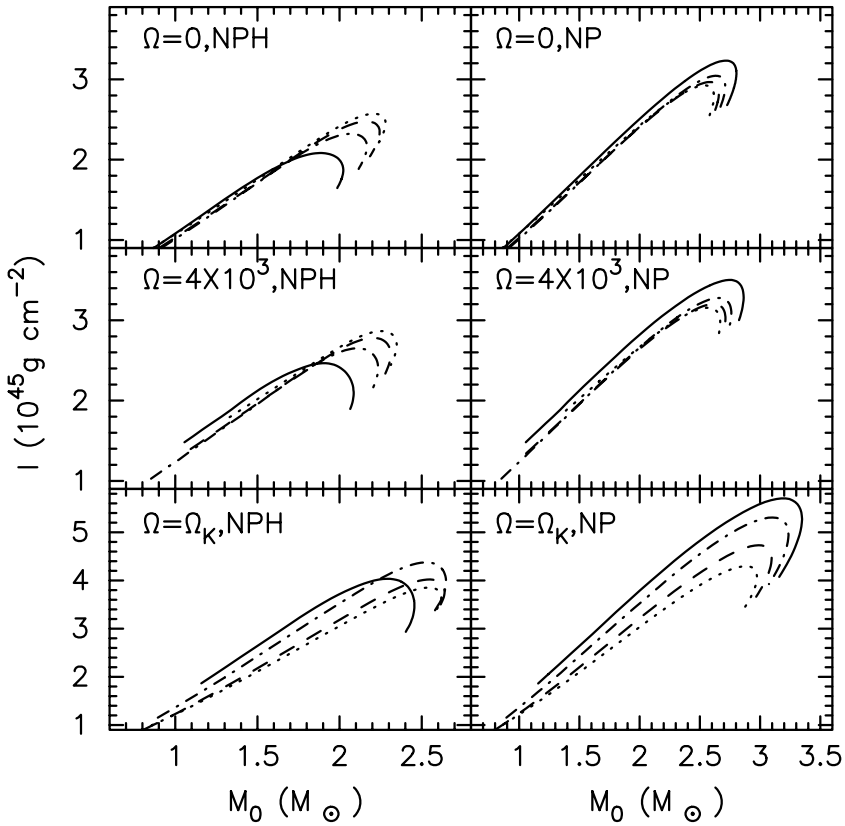

Figure 4. The stellar moment of inertia as a function of the baryonic mass. The solutions traced by the various lines are the same as in Fig. 1.

Figs 3 and 4 show the circumferential equatorial radii and the moments of inertia as a function of the rest mass respectively. In the NP model, if the stellar rest mass M_0 is near the maximum mass, the radii $R_{\rm eq}$ and the moments of inertia I increase as the neutrinos escape and decrease in the NPH model. Evidently, this behaviour is dominated by the change of the EOSs in the stellar core. The trapped neutrinos always make the EOS in the envelope ($n_{\rm B} < n_{\rm env}$) stiffer because of the dominance of the lepton pressure. When the initial mass is small, the PNS first shrinks as the neutrinos escape the envelope, then begins to expand when the pressure of the ρ meson that determines the symmetry energy is comparable to that of the leptons. The change in behaviour is not as significant as what happens to the radii, because the gravitational mass decreases as the neutrinos escape the core. In some sense, this compensates the decrease of the radius.

3 ROTATIONAL EVOLUTION OF PNSS

As investigated in the above section, the global structure of the PNS changes in different ways as the neutrinos escape depending on whether hyperons exist in the core. This may affect the rotational evolution of the PNS. During the evolution of the PNS, the baryonic mass is fixed, if there is no accretion. Neglecting the loss of angular momentum due to the radiation of gravitational and electromagnetic waves, the loss of the total angular momentum of the PNS only results from the emission of the neutrinos. To show how the loss of angular momentum carried away by the neutrinos affects the rotational evolution, we also assume that the neutrinos do not carry any angular momentum as they escape. As emphasized in Section 1, it is a formidable work to keep trace of the loss of angular momentum rigorously during the Kelvin–Helmholtz epoch. In our scenario, we assume that all emitted neutrinos escape from the surface of the neutrino ellipsoid [$r = r_{\rm s}(\theta)$]. Before their escape, they are coupled to the dynamical motion of the fluid. As the neutrinos decouple from the dynamical motion of the fluid, they carry energy and angular momentum away from the star, which lead to the decrease of the gravitational mass and the total angular momentum. Substituting the EOS of the emitted neutrinos at the surface of the neutrino ellipsoid $p_\nu = (1/3)\epsilon_\nu$ and $\epsilon_\nu = \epsilon_0\delta[r - r_{\rm s}(\theta)]$ into equations (4)–(5), we get the ratio (λ) of the lost gravitational mass (ΔM) to the lost angular momentum (ΔJ):

$$\lambda = \lambda(\epsilon_{\rm c}, \Omega; f_{\nu_{\rm e}}) = \frac{\Delta J}{\Delta M} = \frac{\int e^{2\alpha+\gamma}\{[(\epsilon+P)/(1-v)](1+v^2+2r\sin\theta\omega e^{-\rho}v)+2P\}r^2|_{r=r_{\rm s}}\sin\theta\,{\rm d}\theta}{\int e^{2\alpha+\gamma-\rho}[(\epsilon+P)v/(1-v^2)]r^3|_{r=r_{\rm s}}\sin^2\theta\,{\rm d}\theta}. \quad (6)$$

The other trivial constraint comes from the conservation of the baryon mass

$$M_0 = M_0(\epsilon_{\rm c}, \Omega; f_{\nu_{\rm e}}). \quad (7)$$

Based on equations (6)–(7), given the fraction of the trapped neutrinos $f_{\nu_{\rm e}}$, the rotational properties of the PNS can be determined. Changing $f_{\nu_{\rm e}}$ from 1 to 0, the evolutionary sequences of the PNS are obtained. The total lost angular momentum is probably bounded from above by our assumption that all of the neutrinos emerge from the surface of the neutrino ellipsoid. If a conclusion is qualitatively correct in both our model for considering the loss of angular momentum from the PNS and the contrasting model in which the angular momentum of the PNS is constant, it is likely to keep in future rigorous simulations.

To study the evolutionary sequences of rotating PNSs with different interior components, we choose five models to describe the properties of PNSs at the beginning of Kelvin–Helmholtz epoch: the model properties are summarized in Table 1. Fig. 5 shows the stellar circumferential equatorial radii and moments of inertia as a function of neutrino fraction. For the NP model, the radii decrease first mainly because the EOSs of the subnuclear density matter in the stellar envelope become softer as the neutrinos escape. The radii then increase mainly because the EOS of the dense matter in the stellar core becomes stiffer, as contribution from symmetry energy increases. For the NPH model, the radii keep decreasing because both the decrease of the neutrino pressure and the appearance of more and more hyperons in the stellar core make the EOS softer. If $M_0 = 1.5\,{\rm M}_\odot$, hyperonic matter does not appear in the stellar core at all. If $M_0 = 2.2\,{\rm M}_\odot$, the PNS is metastable and it

Table 1. Properties of rigidly rotating PNSs before deleptonization. Their initial angular velocity is taken to be 4000 $\rm s^{-1}$ as an illustration. The hyperon models are labelled as NPH, while the nucleon models are labelled as NP. The entries in the table are: baryon mass, M_0; gravitational mass, M; circumferential equatorial radius, $R_{\rm eq}$; polar radius, $R_{\rm p}$; breakup frequency, $\Omega_{\rm K}$; and central density, $\rho_{\rm c}$. For comparison, the corresponding properties of non-rotating NSs with the same baryon masses are also listed in the right side. The listed quantities include: gravitational mass, M; circumferential radius, R; Keplerian frequency, $\Omega_{\rm K}$; and central density, $\epsilon_{\rm c}$.

Model	M_0	$\Omega = 4000\,{\rm s^{-1}}$ ($Y_{\rm L_e} = 0.4$)					$\Omega = 0$ ($Y_\nu = 0$)			
	($\rm M_\odot$)	M ($\rm M_\odot$)	$R_{\rm eq}$ (km)	$R_{\rm p}$ (km)	$\Omega_{\rm K}$ ($\rm s^{-1}$)	$\epsilon_{\rm c}$ ($10^{15}\,{\rm g\,cm^{-3}}$)	M ($\rm M_\odot$)	R (km)	$\Omega_{\rm K}$ ($\rm s^{-1}$)	$\epsilon_{\rm c}$ ($10^{15}\,{\rm g\,cm^{-3}}$)
	1.5	1.43	18.2	14.2	4331	0.62	1.38	13.6	5084	0.58
NP	2.0	1.85	15.5	13.6	5465	0.83	1.78	13.5	5810	0.76
	2.2	2.00	14.8	13.3	5924	0.96	1.94	13.4	6110	0.86
	1.5	1.43	18.2	14.2	4332	0.62	1.38	13.5	5084	0.65
NPH	2.0	1.85	15.4	13.6	5466	0.85	1.78	12.2	5867	1.60
	2.2	2.00	14.7	13.3	5926	1.08	–	–	–	–

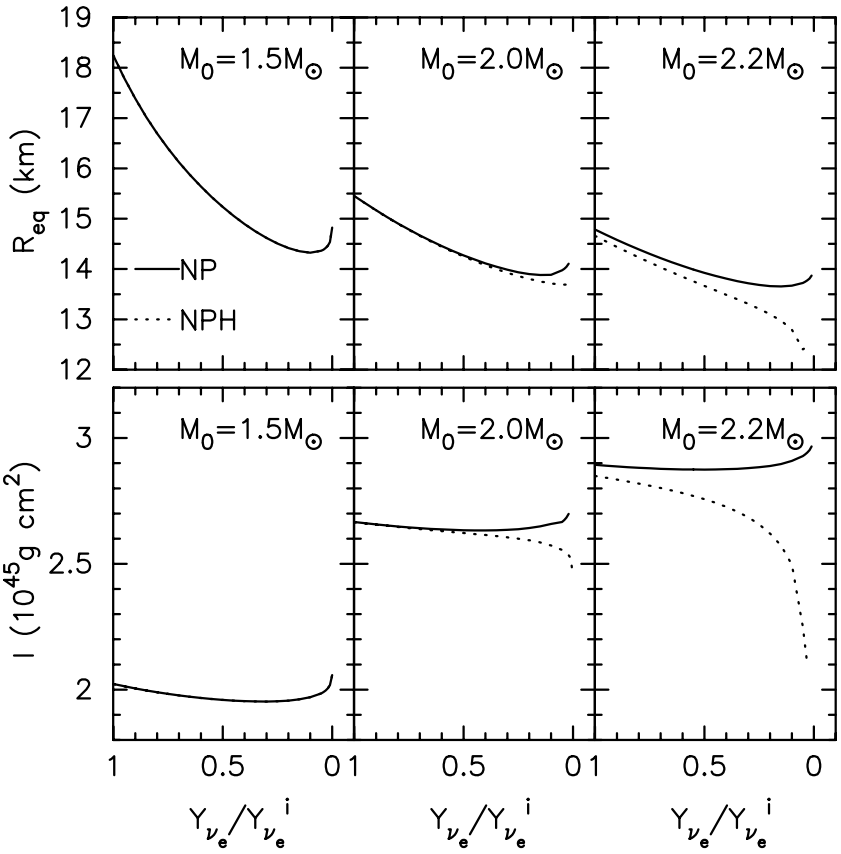

Figure 5. The evolution of the stellar circumferential equatorial radii (upper panels) and the moment of inertia (lower panels) with the escape of the neutrinos at the different fixed rest masses $M_0 = 1.5, 2.0, 2.2\,\mathrm{M}_\odot$. Dotted lines are the results for the PNS with hyperons and solid lines the PNS without hyperons. The initial spin is taken to be $\Omega = 4000\ \mathrm{s}^{-1}$.

collapses to a black hole at the end of the Kelvin–Helmholtz epoch. The evolution of the total moment of inertia is very similar to that of the radii.

The loss of the gravitational mass and the total angular momentum are shown in Fig. 6. The decrease of M by the end of Kelvin–Helmholtz epoch is approximately $0.04\,\mathrm{M}_\odot$ and that of J is approximately $4 \times 10^{47}\ \mathrm{g\,cm^2\,s^{-1}}$ (∼4–5 per cent of their initial values). Neither are sensitive to the initial stellar mass.

Fig. 7 shows how the rotational frequency changes as the neutrinos escape in the NPH and NP model. Early in the Kelvin–Helmholtz epoch, as neutrinos escape the envelope, the PNS always shrinks independently of the presence of hyperons. If the loss of the stellar angular momentum is ignored, the star spins up (see the dotted lines in Fig. 7). The EOS of the subnuclear density material affects the rotational evolution of a PNS significantly (Cheng, Yuan & Zhang 2002). Later in the evolution, roughly speaking, for the NPH model, the PNS spins up with the EOS in the stellar core becoming softer; while for the NP model, the PNS spins down with the EOS in the stellar core becoming stiffer. For $M = 2.0\,\mathrm{M}_\odot$, at the early stage of the evolution, the NPH spins down. Even though the increased number of hyperons makes the EOS softer and the star contract, the loss of the stellar angular momentum tries to make the star slow down. These two effects compete with each other, the spin-down results from the loss of the stellar angular momentum. If the PNS is metastable, the star keeps spinning up significantly, and then collapses to a black hole at the end of its life. It is clearly shown in Fig. 7 that even though the escaped neutrinos carry away some of the angular momentum which decreases the rotational frequency of the PNS, the effect of the change of the global structure due to the escape of the neutrinos dominates the stellar rotational evolution.

The change of the rotational frequencies of the PNS after the neutrinos escape would change the initial distribution of the periods of NSs. Assuming the distribution at the beginning of the Kelvin–Helmholtz epoch is uniform between zero and the Keplerian frequency (∼5465 s^{-1} for $M_0 = 2.0\,\mathrm{M}_\odot$), the new distribution is shown in Fig. 8. For PNSs without hyperons, the range of the periods is somewhat narrower than before, but roughly speaking, the distribution is still almost uniform. For the PNS with hyperons, a significant number of slowly rotating PNSs shift to higher spins; consequently, the presence of hyperonic matter at the centre of NSs will skew the distribution of initial spin periods toward shorter periods.

It should be emphasized that we ignore the thermal effects, that is, we do not consider the influence of mantle contraction which lasts for about 0.5 s. Therefore, our investigation can be understood as study of the rotational evolution starting after this stage. On the other hand, as argued in Section 2.1, for $n_{\mathrm{env}} = 6 \times 10^{-4}\ \mathrm{fm}^{-3}$ we choose, the mass of the mantle is small, and the contribution of the mantle to the total moment of inertia can be neglected. For larger values of n_{env}, such as $n_{\mathrm{env}} = 5 \times 10^{-3}\ \mathrm{fm}^{-3}$ (Goussard et al. 1997), the moment of inertia

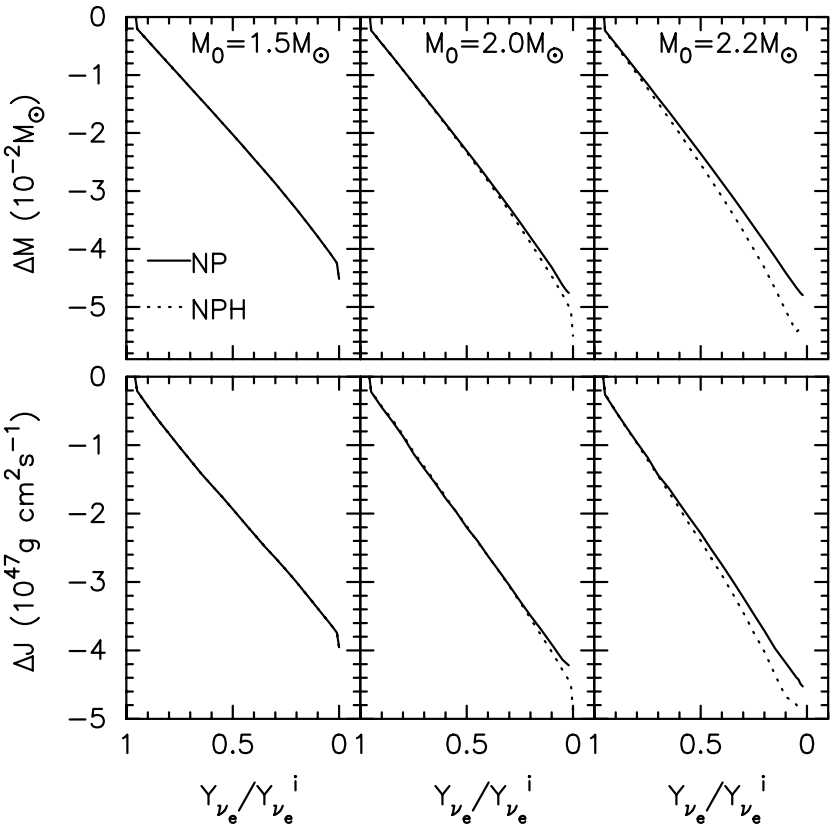

Figure 6. The loss of the gravitational mass (upper panels) and the angular momentum (lower panels) due to the escape of neutrinos. The line symbols are the same as Fig. 5.

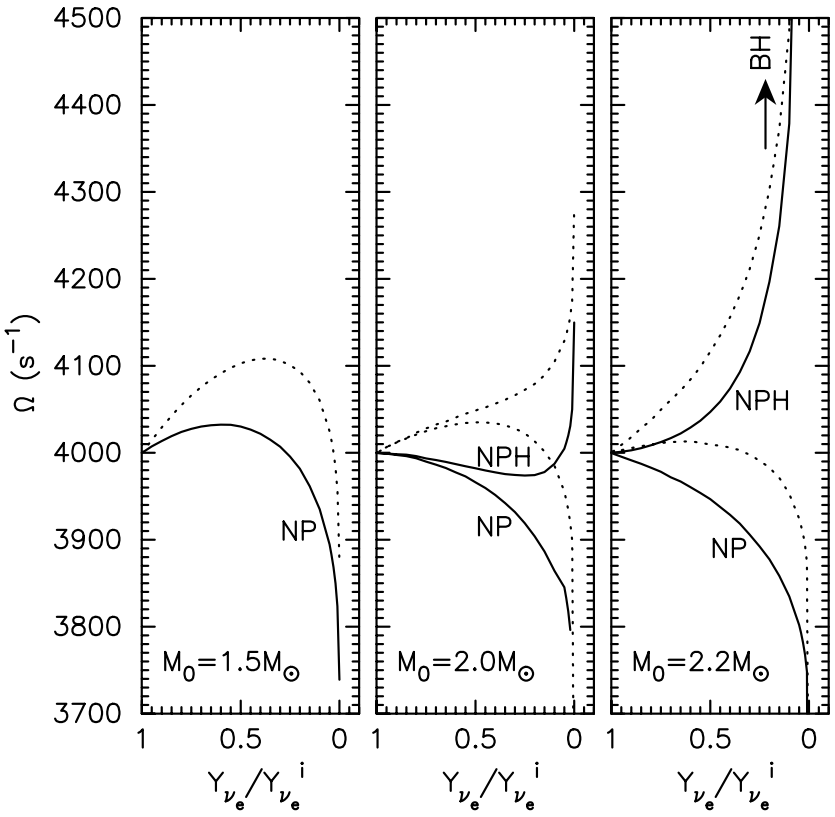

Figure 7. The evolution of the rotation frequency of a PNS with hyperons or not at the different fixed rest masses of the star, $M_0 = 1.5, 2.0, 2.2\,\mathrm{M}_\odot$. The dotted lines represent the corresponding results for the cases in which the stellar angular momentum carried away by the escaped neutrinos is ignored.

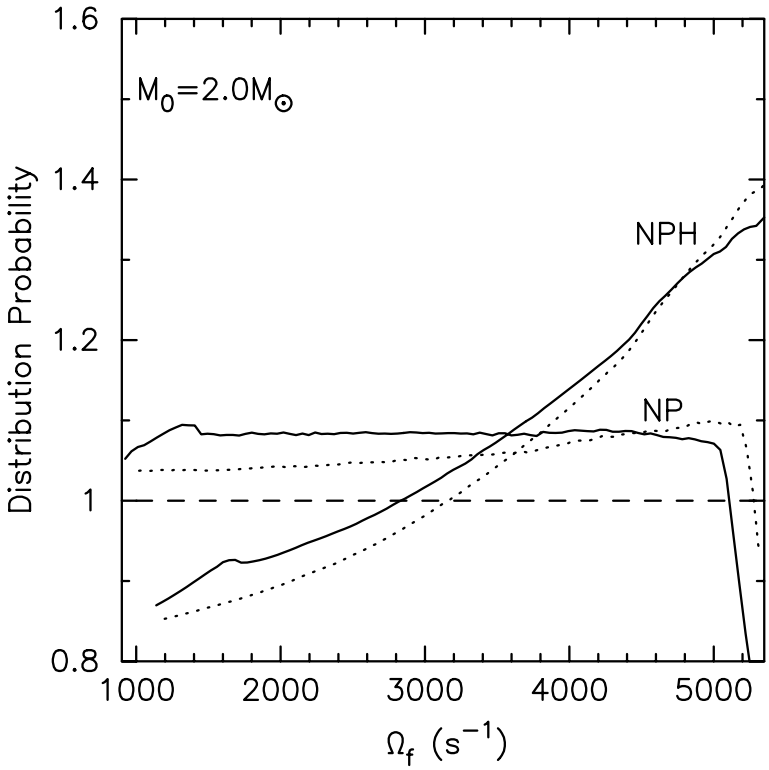

Figure 8. The distribution probability (arbitrary units) of the rotation frequencies of the PNSs whose rest mass is $2.0\,M_\odot$ at the end of the Kelvin–Helmholtz epoch. The dotted lines represent the corresponding results for the cases in which the stellar angular momentum carried away by the escaped neutrinos is ignored and the dashed line represents the assumed uniform distribution of the initial spin periods.

of the hot envelope can no longer be neglected, the mantle contraction might dominate the rotational evolution of PNSs regardless of the interior components; therefore, the spin-up of PNSs after their Kelvin–Helmholtz epoch in the previous works mainly results from the mantle contraction (Goussard et al. 1997; Villain et al. 2004).

4 CONCLUSION AND DISCUSSION

In this paper, we investigate the evolution of rigidly rotating PNSs that contain only nucleons with that of PNSs which contain hyperonic matter at zero temperature in full general relativity. It is found that a PNS contracts at the early stage of its evolution as the trapped neutrinos escape. During this stage the contribution of leptons to the pressure in the stellar envelope dominates. This conclusion is independent of the interior composition. If the loss of the stellar angular momentum is small, the star should spin up. However, under our liberal assumption for the loss of the angular momentum due to neutrinos, the star slows down at this contracting stage. As the neutrinos continue to escape, the evolution of the PNS mainly depends on the changing behaviour of the EOS of the dense matter in the stellar core; therefore, it differs in the two different models. A PNS that contains only nucleons stops contracting and begins to expand because the EOS becomes stiffer as neutrinos escape from the core. PNSs that contain hyperonic matter keep shrinking and their spin frequency increases because the EOS becomes softer with the escape of the neutrinos. At the end of the evolution, for PNSs without hyperons, the range of the spin periods becomes a little bit narrower than the initial one. However, the shape of the distribution of the spin periods is very similar to that of the initial distribution. For PNSs with hyperons, the distribution of the initial spin periods is skewed significantly towards shorter periods. If a PNS is metastable, it keeps spinning up significantly on the neutrino diffusion time-scale before it collapses to a black hole.

In addition to the hyperonic matter, other exotic states, such as quark matter, kaon condensation and others might exist in the stellar core. Because the neutrino trapping makes the onset of these exotic states that contain negatively charged particles take place at the higher baryon number density, a PNS with such an exotic composition might spin up as the neutrinos escape. This characteristic phenomenon might be common among them.

In this work, the effect of the temperature is ignored. Certainly regardless of the interior composition, heat introduces another energy source, which would make the EOS stiffer than in the zero temperature case. In the inner core, temperature has little effect on the global properties such as stellar masses, luminosities, average temperatures of average lepton content and so on. However, in the outer layers, the EOS becomes much stiffer than in the zero-temperature case, therefore, the initial stellar radii are approximately 50–100 km. Because, in our consideration, we choose $n_{\rm env} = 6 \times 10^{-4}$ fm^{-3} (Goussard et al. 1997), the gravitational mass of the mantle is only approximately $\sim 6 \times 10^{-4}\,M_\odot$, therefore, the ratio of the moment of inertia of the hot envelope to the total one is only approximately 1 per cent. In calculating the

evolution of the angular velocity, the effects of the mantle contraction can be neglected. At the late stage of the stellar evolution, the cooling of the PNS cannot change the results we obtain qualitatively, because the change of the chemical equilibrium among the interior particles dominates the change of the EOS. Of course, if further investigations show that $n_{\rm env}$ is much greater than the value we choose, some results we obtain in this paper (e.g. such as the spin-down of PNSs, which include solely nucleons) will change. If so, our work traces qualitatively the evolutionary behaviour of PNSs, starting from the end of the stellar mantle contraction.

We do not investigate the evolution of differentially rotating PNSs. According to Villain et al. (2004), differential rotation increases the central angular velocity up to 5–10 times relative to the case of rigid rotation. In our opinion, the corresponding central density decreases significantly and the properties of rapidly rotating PNSs are mainly determined by the EOS of the lower density nuclear matter, under which the exotic states such as hyperons do not emerge. As the neutrinos escape, generally the EOS becomes softer, so the star shrinks and spins up.

In principle, the rotation period of a PNS could be observed by a ground-based gravitational radiation detector, such as the Laser Interferometer Gravitational Wave Observatory (LIGO). Fryer, Holz & Hughes (2002) examine several avenues for gravitational wave emission from core collapse. If the core forms a bar or breaks in two, the analysis that we have presented here is inapplicable because we have assumed that the core remains axisymmetric (equation 3). Furthermore, the third mode that they considered is the ringdown of the black hole; in this case, the PNS stage is no longer visible. However, they also have estimated the role that *r* modes may play in gravitational wave generation (Ho & Lai 2000). The frequency of the observed gravitational radiation reflects the spin frequency of the PNS, so the waveform would reveal the internal structure of the PNS as long as fallback did not strongly affect the spin of the core during the Kelvin–Helmholtz epoch. It is unclear whether *r* modes will have a chance to grow during this early epoch (Fryer et al. 2002), but if they do LIGO-II could detect gravitational radiation from supernovae within 10 Mpc.

The decrease of the gravitational mass of PNS is due to the release of thermal neutrinos; therefore, a huge energy ($\sim 0.01\,{\rm M}_\odot$) is released in the form of high energy neutrinos during the Kelvin–Helmholtz epoch. If the neutrino flux from the PNS is modulated with the stellar rotation, a neutrino telescope might observe temporal structure at the stellar period: this could provide strict constraints on models of dense matter. The typical energy of the emitted neutrinos is a few MeV (Arnett et al. 1989). 20 neutrinos were detected from SN1987A (Bionta et al. 1987; Hirata et al. 1987) over approximately a 10-s interval. Currently, the total sensitivity of detectors sensitive to supernova neutrinos is 30 times larger than in 1987, so one would expect to detect approximately 15 000 neutrinos from a galactic supernova. Ransom, Eikenberry & Middleditch (2002) give straightforward formulae to estimate the minimum pulsed fraction detectable with a given certainty from a sample of arrival times. If we assume that the spin frequency of the PNS lies between 0 and 1500 Hz and that the spin may vary by 200 Hz during the 10-s duration of the neutrino burst, a blind search for the spin frequency and its evolution would require approximately 3×10^7 trials. If one wants to detect a signal with a false alarm probability of P_0, the minimum sinusoidal pulsed fraction that one could detect is

$$f_{\rm p} = 2\left[\frac{\ln(N_{\rm trial}/P_0) - 1}{N}\right]^{1/2} = 0.08 \tag{8}$$

for a false alarm probability of 10^{-3} and 15 000 detected neutrinos. Because the expected change in frequency is small compared with the expected spin frequency, an unaccelerated search only does marginally better with a minimum detectable pulsed fraction of 0.06. Although these pulsed fractions are several times larger than required for pulsar kicks (e.g. Spruit & Phinney 1998; Arras & Lai 1999), Earthbound neutrino detectors are most sensitive to neutrinos in the Wien tail of the thermal distribution where the pulsed fraction will be larger than the momentum anisotropy.

A third observational probe of these models is the distribution of initial periods of NSs. This may be obtained from the distribution of current spin periods of radio pulsars along with an independent estimate of the ages of the NSs. One must assume that only magnetic dipole radiation has contributed to the spin-down and furthermore that the standard model for magnetic dipole radiation is correct (Kaspi & Helfand 2002). If gravitational radiation is important, then such estimates of the initial spin distribution probe the gravitational radiation epoch (see Owen et al. 1998; Ho & Lai 2000; Arras et al. 2003; Watts & Andersson 2002, for a few viewpoints) rather than the PNS epoch discussed here. Only a few NSs have a good estimates of their initial periods, which are typically an order of magnitude longer than the Kepler period. If the emission of gravitational radiation is not important to the spin evolution of NSs, this would argue against a skewed distribution of NS initial spins; however, so few NSs have estimates of their initial periods and the contribution of gravitational radiations is uncertain, so it is premature to make any definite conclusions.

The most spectacular manifestation of the rotational evolution of a PNS would be the formation and subsequent collapse of a metastable stellar core. How the core collapses into a black hole and the observable consequences of that collapse are beyond the scope of this paper. We will examine the process in a subsequent paper. For a PNS that rotates rapidly, an important issue is whether the entire PNS can collapse on a dynamical time or portions of the star cannot fall directly into the black hole and form an accretion disc, which evolves on a viscous time-scale. This could provide a detailed model of the central engines of collapsars, a successful explanation of gamma-ray bursts (MacFadyen, Woosley & Heger 2001).

We have studied the structure of rapidly rotating axisymmetric PNSs using a fully general relativistic treatment of the stellar structure and RMFT to model the EOS of dense matter. We have contrasted the spin evolution of normal PNSs with hyperonic PNSs. In general, the evolution PNSs with other exotic species will be similar to that of hyperonic NSs. We confirmed the previous finding that hyperonic PNSs can be metastable; that is, the maximum mass of a stable hyperonic PNS decreases as the neutrinos escape (Pons et al. 1999). As neutrinos begin to escape the core of a hyperonic PNS, the core spins up. The metastable PNS spins up as it begins to collapse to a black hole. This contrasts with the behaviour of a normal PNS. As neutrinos stream out of the core of a normal PNS, the EOS stiffens, the core expands and

spins down. This spin evolution leaves a signature on both the neutrino emission and gravitational radiation from the stellar collapse that might be observable from nearby supernovae. Finally, if the processes leading to the formation of hyperonic and normal PNSs are similar, we would expect the hyperonic NSs initially to spin faster than normal NSs.

ACKNOWLEDGMENTS

It is a great pleasure for us to thank the anonymous referee for her/his constructive suggestions that were helpful in improving this manuscript significantly. We would like to give thanks for the discussions with Prof. Ramesh Narayan, Prof K. S. Cheng, Prof J. L. Zhang, Dr Scott Ransom and Dr John Bahcall. Y-FY acknowledges the hospitality of Harvard-Smithsonian Center for Astrophysics. Y-FY is partially supported by the Special Funds for Major State Research Projects and the National Natural Science Foundation (10233030). Support for JSH was provided by the National Aeronautics and Space Administration through Chandra Postdoctoral Fellowship Award Number PF0-10015 issued by the Chandra X-ray Observatory Center, which is operated by the Smithsonian Astrophysical Observatory for and on behalf of NASA under contract NAS8-39073.

REFERENCES

Akiyama S., Wheeler J. C., Meier D. L., Lichtenstadt I., 2003, ApJ, 584, 954
Arnett W. D., Bahcall J. N., Kirshner R. P., Woosley S. E., 1989, ARA&A, 27, 629
Arras P., Lai D., 1999, ApJ, 519, 745
Arras P., Flanagan E. E., Morsink S. M., rin Schenk A. K., Teukolsky S. A., Wasserman I., 2003, ApJ, 591, 1129
Bionta R. M., Blewitt G., Bratton C. B., Casper, D., Ciocio A., 1987, Phys. Rev. Lett., 58, 1494
Boguta J., Bodmer A. R., 1977, Nucl. Phys. A, 292, 413
Bombaci I., Prakash M., Prakash M., Ellis P. J., Lattimer J. M., Brown G. E., 1995, Nucl. Phys. A, 583, 623
Burrows A., 2000, Nat, 403, 727
Burrows A., Lattimer J. M., 1986, ApJ, 307, 178
Burrows A., Hayes J., Fryxell B. A., 1995, ApJ, 450, 830
Cheng K. S., Yuan Y. F., Zhang J. L., 2002, ApJ, 564, 909
Chin S. A., 1977, Ann. Phys., 108, 301
Chubarian E., Grigorian H., Poghosyan G., Blaschke D., 2000, A&A, 357, 968
Fryer C. L., Heger A., 2000, ApJ, 541, 1033
Fryer C. L., Holz D. E., Hughes S. A., 2002, ApJ, 565, 430
Glendenning N. K., 1992, Phys. Rev. D, 46, 4161
Glendenning N. K., 2000, Compact Stars, Nuclear Physics, Particle Physics, and General Relativity. Springer, New York
Glendenning N. K., Moszkowski S. A., 1991, Phys. Rev. Lett., 67, 2414
Glendenning N. K., Pei S., Weber F., 1997, Phys. Rev. Lett., 79, 1603
Goussard J. O., Haensel P., Zdunik J. L., 1997, A&A, 321, 822
Goussard J.-O., Haensel P., Zdunik J. L., 1998, A&A, 330, 1005
Hartle J. B., 1967, ApJ, 150, 1005
Hartle J. B., Thorne K. S., 1968, ApJ, 153, 807
Hashimoto M., Oyamatsu K., Eriguchi Y., 1994, ApJ, 436, 257
Heger A., Langer N., Woosley S. E., 2000, ApJ, 528, 368
Hirata K., Kajita T., Koshiba M., Nakahata M., Oyama Y., 1987, Phys. Rev. Lett., 58, 1490
Ho W. C. G., Lai D., 2000, ApJ, 543, 386
Janka H., Kifonidis K., Rampp M., 2001, in Beig R. et al., eds, Lecture Notes in Physics, Vol. 578. Springer Verlag, Berlin, p. 333
Kaspi V. M., Helfand D. J., 2002, in Slane P. O., Gaensler B. M, eds, ASP Conf. Ser. Vol. 271, Neutron Stars in Supernova Remnants. Astron. Soc. Pac., San Francisco, p. 3
Keil W., Janka H.-T., 1995, A&A, 296, 145
Komatsu H., Eriguchi Y., Hachisu I., 1989a, MNRAS, 237, 355
Komatsu H., Eriguchi Y., Hachisu I., 1989b, MNRAS, 239, 153
Lorenz C. P., Ravenhall D. G., Pethick C. J., 1993, Phys. Rev. Lett., 70, 379
MacFadyen A. I., Woosley S. E., Heger A., 2001, ApJ, 550, 410
Müller H., Serot B. D., 1996, Nucl. Phys. A, 606, 508
Owen B. J., Lindblom L., Cutler C., Schutz B. F., Vecchio A., Andersson N., 1998, Phys. Rev. D, 58, 84020
Pons J. A., Reddy S., Prakash M., Lattimer J. M., Miralles J. A., 1999, ApJ, 513, 780
Pons J. A., Miralles J. A., Prakash M., Lattimer J. M., 2001a, ApJ, 553, 382
Pons J. A., Steiner A. W., Prakash M., Lattimer J. M., 2001b, Phys. Rev. Lett., 86, 5223
Prakash M., Cooke J. R., Lattimer J. M., 1995, Phys. Rev. D, 52, 661
Prakash M., Bombaci I., Prakash M., Ellis P. J., Lattimer J. M., Knorren R., 1997, Phys. Rep., 280, 1
Ransom S. M., Eikenberry S. S., Middleditch J., 2002, AJ, 124, 1788
Reddy S., Prakash M., Lattimer J. M., 1998, Phys. Rev. D, 58, 13009
Romero J. V., Diaz Alonso J., Ibanez J. M., Miralles J. A., Perez A., 1992, ApJ, 395, 612
Serot B. D., 1979, Phys. Lett. B, 86, 146
Serot B. D., Walecka J. D., 1986, Adv. Nucl. Phys., 16, 1
Spruit H. C., Phinney E. S., 1998, Nat, 393, 139
Stergioulas N., 1998, Living Rev. Relativity, 1, 8
Stergioulas N., Friedman J. L., 1995, ApJ, 444, 306

Strobel K., Schaab C., Weigel M. K., 1999, A&A, 350, 497
Sumiyoshi K., Ibáñez J. M., Romero J. V., 1999, A&AS, 134, 39
Takatsuka T., Nishizaki S., Hiura J., 1994, Prog. Theor. Phys., 92, 779
Thompson C., Duncan R. C., 1993, ApJ, 408, 194
Vidaña I., Bombaci I., Polls A., Ramos A., 2003, A&A, 399, 687
Villain L., Pons J. A., Cerdá-Durán P., Gourgoulhon E., 2004, A&A, 418, 283
Walecka J. D., 1974, Ann. Phys., 83, 491
Watts A. L., Andersson N., 2002, MNRAS, 333, 943
Weber F., Glendenning N. K., 1992, ApJ, 390, 541
Yuan Y. F., Zhang J. L., 1999, ApJ, 525, 950

APPENDIX A: DESCRIPTION OF THE DENSE MATTER

In the framework of relativistic field theory, the interaction between nucleons and hyperons is mediated by the exchange of three meson fields, σ, ω and ρ mesons. The coupling constants and meson masses can be algebraically related to the bulk properties of symmetric nuclear matter (Glendenning 2000). The Lagrangian of the hadrons is given by

$$\begin{aligned}\mathcal{L} = &\sum_i \overline{\psi}_i \left[i\gamma_\mu \left(\partial^\mu + i g_{\omega i}\omega^\mu + i\frac{g_{\rho i}}{2}\boldsymbol{\tau}\cdot\boldsymbol{\rho}^\mu \right) - (m_i - g_{\sigma i}\sigma) \right]\psi_i \\ &+ \frac{1}{2}\left(\partial_\mu\sigma\partial^\mu\sigma - m_\sigma^2\sigma^2\right) - U(\sigma) \\ &- \frac{1}{4}\omega_{\mu\nu}\omega^{\mu\nu} + \frac{1}{2}m_\omega^2\omega_\mu\omega^\mu \\ &- \frac{1}{4}\boldsymbol{\rho}_{\mu\nu}\cdot\boldsymbol{\rho}^{\mu\nu} + \frac{1}{2}m_\rho^2\boldsymbol{\rho}_\mu\cdot\boldsymbol{\rho}^\mu, \end{aligned} \tag{A1}$$

where

$$\omega_{\mu\nu} = \partial_\mu\omega_\nu - \partial_\nu\omega_\mu, \tag{A2}$$

$$\boldsymbol{\rho}_{\mu\nu} = \partial_\mu\boldsymbol{\rho}_\nu - \partial_\nu\boldsymbol{\rho}_\mu + g_{\rho n}\boldsymbol{\rho}_\mu\times\boldsymbol{\rho}_\nu. \tag{A3}$$

Throughout this paper, we will use the set of natural units where $\hbar = c = 1$ unless noted otherwise. Here ψ_i, σ, ω and $\boldsymbol{\rho}$ denote the fields of the baryon of species i ($i = n$, p, Λ, Σ^-, Σ^0, Σ^+, Ξ^-, Ξ^0), the mesons σ, ω and ρ with the masses of m_i, m_σ, m_ω, m_ρ, respectively. The constants $g_{\sigma i}$, $g_{\omega i}$, $g_{\rho i}$ are coupling constants for interactions between mesons and baryons. $\boldsymbol{\tau} = (\tau_1, \tau_2, \tau_3)$ denotes the 2×2 Pauli isospin matrices and the dot and cross products are calculated over isospin space. The potential of the self-interaction of the scalar field, which reads

$$U(\sigma) = \frac{1}{3}bm_n(g_{\sigma n}\sigma)^3 + \frac{1}{4}c(g_{\sigma n}\sigma)^4, \tag{A4}$$

is introduced to produce reasonable incompressibility of nuclear matter (Boguta & Bodmer 1977). Here, the coefficients b and c denote self-coupling constants for the σ meson field.

The dynamical equations of nucleons and mesons can be derived from the above Lagrangian. Generally, these equations are coupled. Applying the RMFT approximation (Walecka 1974), the dynamical equations are decoupled: they are,

$$\mu_i = g_{\omega i}\omega_0 + g_{\rho i}\rho_{03}I_{3i} + \sqrt{k^2 + m_i^{*2}}, \tag{A5}$$

$$m_\sigma^2\sigma = g_{\sigma i}n_{si} - \frac{\partial U(\sigma)}{\partial\sigma}, \tag{A6}$$

$$\omega_0 = \sum_i \frac{g_{\omega i}}{m_\omega^2}n_i, \tag{A7}$$

$$\rho_{03} = \sum_i \frac{g_{\rho i}}{m_\rho^2}I_{3i}n_i. \tag{A8}$$

Here, μ_i is the chemical potentials of baryons, I_{3i} is the third component of isospin for the baryons and $m_i^* = m_i - g_{\sigma i}\sigma$ are the effective masses of baryons. Finally, the scalar density $n_{si} \equiv \langle\overline{\psi}\psi\rangle$ is defined as

$$n_{si} = \frac{2}{\pi^2}\int_0^{k_i^{\rm F}} \frac{m_i^*}{\sqrt{k^2 + (m_i^*)^2}}k^2\,{\rm d}k, \tag{A9}$$

where $k_i^{\rm F}$ are the Fermi momenta of baryons. The condition of chemical equilibrium between baryons and leptons is given by

$$\mu_i = b_i\mu_n - q_i\tilde{\mu}_l, \tag{A10}$$

where b_i is the baryon number of particle i and q_i is its charge. For the neutrino-free case, $\tilde{\mu_l} = \mu_l$, for the trapped-neutrino case, $\tilde{\mu_l} = \mu_l - \mu_{\nu_l}$. Here, μ_l ($l = {\rm e}^-$, μ^-) are the chemical potentials of the leptons. Because neutrinos are trapped, the lepton number per baryon $Y_{{\rm L}_l}$ of each

flavour must be conserved on dynamical time-scales,

$$Y_{\mathrm{L}_l} = Y_l + Y_{\nu_l} = \text{constant}. \tag{A11}$$

Studies of the gravitational collapse calculations of the core of a massive star indicate that $Y_{\mathrm{L_e}} \simeq 0.4$ (Prakash et al. 1997). In addition, because no muons appear when neutrinos become trapped, $Y_{\mathrm{L}_\mu} = 0$. During the Kelvin–Helmholtz epoch, Y_{ν_e} changes from its initial value to zero. Therefore, if the chemical potentials of neutrons and electrons are known, the fields of the mesons σ, ω and ρ can be solved numerically, and then the momenta of all the baryons can be determined at the same time. Given the baryon number density n_B, the additional condition, charge neutrality, is needed to determine μ_n and μ_e self-consistently.

According to the standard procedure of RMFT theory (Walecka 1974), the energy density and the pressure of the baryons can be obtained:

$$\epsilon_\mathrm{B} = \frac{1}{2}m_\sigma^2\sigma^2 + \frac{1}{2}m_\omega^2\omega_0^2 + \frac{1}{2}m_\rho^2\rho_{03}^2 + \sum_i \frac{1}{\pi^2}\int_0^{p_i^\mathrm{F}} \sqrt{p^2 + m_i^*}\, p^2\, \mathrm{d}p, \tag{A12}$$

$$p_\mathrm{B} = -\frac{1}{2}m_\sigma^2\sigma^2 + \frac{1}{2}m_\omega^2\omega_0^2 + \frac{1}{2}m_\rho^2\rho_{03}^2 + \sum_i \frac{1}{\pi^2}\int_0^{p_i^\mathrm{F}} \frac{p^4\, \mathrm{d}p}{\sqrt{p^2 + m_i^*}}. \tag{A13}$$

The coupling constants $g_{\sigma N}$, $g_{\omega N}$, $g_{\rho N}$, b, c ($N = n$, p) in RMFT are algebraically related to the bulk properties of symmetric nuclear matter at saturation density. In our calculation, we choose the so-called GM1 set (Glendenning & Moszkowski 1991),

$$\left(\frac{g_{\sigma N}}{m_\sigma}\right)^2 = 11.79, \quad \left(\frac{g_{\omega N}}{m_\omega}\right)^2 = 7.149, \quad \left(\frac{g_{\rho N}}{m_\rho}\right)^2 = 4.411, \quad b = 2.947 \times 10^{-3}, \quad c = -1.07 \times 10^{-3}, \tag{A14}$$

from which the nuclear properties arise as follows: the saturation density, effective mass of nuclear, incompressibility, and binding energy per nucleon $n_0 = 0.153\ \mathrm{fm}^{-3}$, $m^* = 0.7$, $K = 300$ MeV and $B/A = -16.3$ MeV.

At the saturation density, the bulk properties are independent of the hyperon couplings, which could be determined by reproducing the binding of the Λ hyperon in nuclear matter (Glendenning & Moszkowski 1991). It is assumed that all hyperons in the octet have the same coupling, which is expressed in terms of nucleon couplings,

$$x_{\sigma H} = \frac{g_{\sigma H}}{g_{\sigma N}}, \quad x_{\omega H} = \frac{g_{\omega H}}{g_{\omega N}}, \quad x_{\rho H} = \frac{g_{\rho H}}{g_{\rho N}}. \tag{A15}$$

In the GM1 set (Glendenning, Pei & Weber 1997; Glendenning & Moszkowski 1991; Glendenning 2000),

$$x_{\sigma H} = 0.6, \quad x_{\omega H} = x_{\rho H} = 0.653. \tag{A16}$$

This paper has been typeset from a TEX/LATEX file prepared by the author.